

Evolution of magnetic properties in the normal spinel solid solution $\text{Mg}_{1-x}\text{Cu}_x\text{Cr}_2\text{O}_4$

Moureen C. Kemei, Stephanie L. Moffitt, and Ram Seshadri

Materials Department, University of California, Santa Barbara CA 93106

E-mail: kemei@mrl.ucsb.edu

Daniel P. Shoemaker

Material Science Division, Argonne National Laboratory, Argonne IL 60439

Abstract.

We examine the evolution of magnetic properties in the normal spinel oxides $\text{Mg}_{1-x}\text{Cu}_x\text{Cr}_2\text{O}_4$ using magnetization and heat capacity measurements. The end-member compounds of the solid solution series have been studied in some detail because of their very interesting magnetic behavior. MgCr_2O_4 is a highly frustrated system that undergoes a first order structural transition at its antiferromagnetic ordering temperature. CuCr_2O_4 is tetragonal at room temperature as a result of Jahn-Teller active tetrahedral Cu^{2+} and undergoes a magnetic transition at 135 K. Substitution of magnetic cations for diamagnetic Mg^{2+} on the tetrahedral *A* site in the compositional series $\text{Mg}_{1-x}\text{Cu}_x\text{Cr}_2\text{O}_4$ dramatically affects magnetic behavior. In the composition range $0 \leq x \leq \approx 0.3$, the compounds are antiferromagnetic. A sharp peak observed at 12.5 K in the heat capacity of MgCr_2O_4 corresponding to a magnetically driven first order structural transition is suppressed even for small x suggesting glassy disorder. Uncompensated magnetism – with open magnetization loops – develops for samples in the x range $\approx 0.43 \leq x \leq 1$. Multiple magnetic ordering temperatures and large coercive fields emerge in the intermediate composition range $0.43 \leq x \leq 0.47$. The Néel temperature increases with increasing x across the series while the value of the Curie-Weiss Θ_{CW} decreases. A magnetic temperature-composition phase diagram of the solid solution series is presented.

PACS numbers: 75.30.Kz 75.47.Lx 75.50.Ee 75.50.Gg

1. Introduction

Materials with the spinel structure display a wide range of functional properties and are applied as battery electrodes [1], multiferroic materials [2, 3], and catalytic materials. [4] In addition, spinels offer unique opportunities for the exploration of exotic magnetic phenomena. [5, 6, 7] A rich diversity of possible magnetic ground states can be found in materials with the spinel structure. These range from long range ordered ferrimagnetic states, observed in magnetite Fe_3O_4 , to degenerate spin liquid states seen in systems with geometrically frustrated interactions such as $ZnCr_2O_4$. [8] In spinels with the general formula AB_2O_4 , cation A and B sites can both be occupied by magnetic ions. Coupling between the various magnetic ions gives rise to a number of competing exchange pathways and a multitude of possible ground states. Additional complexity arises when antiferromagnetically coupled cations populate the pyrochlore B sublattice in spinels. In this configuration, geometric constraints preclude the realization of a unique ground state resulting in frustrated systems. Slight perturbations of highly degenerate spin liquid states in frustrated magnets can result in a range of novel behavior. [9, 10]

Strongly frustrated three-dimensional pyrochlore B sublattices occur in oxide spinels with a non-magnetic A site and a chromium B site. Cr^{3+} with a $[Ar]3d^3$ electron configuration shows a preference for the octahedral site where crystal field splitting stabilizes a half filled t_{2g} level separated in energy from an empty e_g level. [11, 12] Antiferromagnetic nearest neighbour (NN) interactions between Cr^{3+} ions populating the pyrochlore B sublattice cannot be fully satisfied. Pyrochlore sublattices with antiferromagnetically coupled spins have been shown to result in frustrated Heisenberg spin Hamiltonian expressions where NN interactions alone would not result in a single low energy state even at $T = 0$ K. [13, 14, 15, 16] Given the strongly frustrated Cr^{3+} sublattice, the choice of A site cation can profoundly affect magnetic properties in chromium oxide spinels.

Magnetic ground states depend strongly on the A cation in ACr_2O_4 spinels. Non-magnetic A site (for instance $A = Zn, Mg, Cd$) chromium oxide spinels are highly frustrated. [17] Spin-lattice coupling resolves the large ground state degeneracy by selecting a unique ordered state *via* a spin Jahn-Teller effect at the magnetic ordering temperature. [16] In magnetic A site spinels (for instance $A = Co, Fe, Cu, Mn$), A -O-Cr coupling dominates over frustrated Cr-Cr interactions and non-collinear ferrimagnetic ground states are attained. [18, 19, 20, 21, 22, 23] Understanding changes in interactions due to gradual addition of magnetic ions on the A site of frustrated ACr_2O_4 spinels is important. In this study, we investigate the magnetic properties of the solid solution $Mg_{1-x}Cu_xCr_2O_4$ where the end members $MgCr_2O_4$ and $CuCr_2O_4$ differ both structurally and magnetically.

The canonical geometrically frustrated spinel $MgCr_2O_4$ crystallizes in the cubic space group $Fd\bar{3}m$ at 300 K. The pyrochlore Cr^{3+} sublattice is based on a triangular motif where antiferromagnetic NN Cr-Cr coupling is geometrically frustrated. As a result, the spins in $MgCr_2O_4$ remain disordered far below the theoretical ordering

temperature ($\Theta_{CW} \approx -400$ K).[24, 25] A structural distortion lifts the spin state degeneracy of the pyrochlore Cr^{3+} sublattice at the Néel temperature (T_N) ≈ 12.5 K. The tetragonal space group $I4_1/amd$ has been suggested as the low symmetry crystallographic structure.[26, 27] A sharp peak in heat capacity coincident with the magnetically driven structural transition in $MgCr_2O_4$ denotes the first-order nature of this transition.[28]

The spinel $CuCr_2O_4$ is cubic above 873 K,[29, 30] with Cu^{2+} occupying tetrahedral sites and Cr^{3+} populating octahedral sites. In the cubic phase, tetrahedral crystal field splitting of the d^9 Cu^{2+} energy level results in triply degenerate high lying t_2 subshells and fully occupied low energy e_g subshells.[31] Distortion of the CuO_4 tetrahedra lifts the orbital degeneracy of the t_2 level, and when these distortions are coherent, the symmetry of $CuCr_2O_4$ is lowered from cubic $Fd\bar{3}m$ to tetragonal $I4_1/amd$. [32] Magnetic studies of $CuCr_2O_4$ show that it is ferrimagnetic at 135 K. The magnetic structure in the ordered state is triangular with Cr^{3+} in the 001 planes alligned parallel but at an angle to Cr^{3+} in adjacent planes. Cu^{2+} align antiparallel to the net moment of the Cr^{3+} sublattices forming a magnetic structure comprising triangles of spins.[20]

Previous work has investigated the local and average structural changes in the series $Mg_{1-x}Cu_xCr_2O_4$. [33] These studies show that although local distortions occur for all Cu^{2+} substituted compositions, cooperative structural changes are dependent on x and on temperature. For example, at room temperature, compounds of the series $Mg_{1-x}Cu_xCr_2O_4$ remain cubic on average for $x < 0.43$. Tetragonal average symmetry driven by cooperative Cu^{2+} Jahn-Teller distortions appears in compositions with $x > 0.43$ at 300 K.

We study the effect of introducing magnetic, Jahn-Teller active Cu^{2+} on the non-magnetic A site of $MgCr_2O_4$ on magnetic frustration and on the nature of magnetic interactions. A previous study of the system $Zn_{1-x}Co_xCr_2O_4$ showed that addition of Co^{2+} on the non-magnetic Zn^{2+} site quenched frustration across the series.[34] Here, we explore changes in magnetic behavior as Jahn-Teller active tetrahedral Cu^{2+} induces lattice distortions in addition to adding magnetism on A site of the compounds $Mg_{1-x}Cu_xCr_2O_4$. [33] Novel properties such as intrinsic exchange bias have been shown to exist at phase boundaries.[35] We therefore closely examine the region between the antiferromagnetic and ferrimagnetic phases in $Mg_{1-x}Cu_xCr_2O_4$ for unusual phenomena.

2. Experimental details

Polycrystalline samples of the series $Mg_{1-x}Cu_xCr_2O_4$ ($x = 0, 0.1, 0.2, 0.43, 0.47, 0.6, 0.8,$ and 1) were prepared through calcination of nitrate precursors as reported by Shoemaker and Seshadri.[33] The samples were structurally characterized by laboratory x-ray diffraction using a Philips X'pert diffractometer with $Cu-K\alpha$ radiation. Phase purity was confirmed in selected compositions using high-resolution synchrotron powder x-ray diffraction collected at the 11-BM beamline at the Advanced Photon Source. Some of the samples have also been previously characterized by time-of-flight neutron

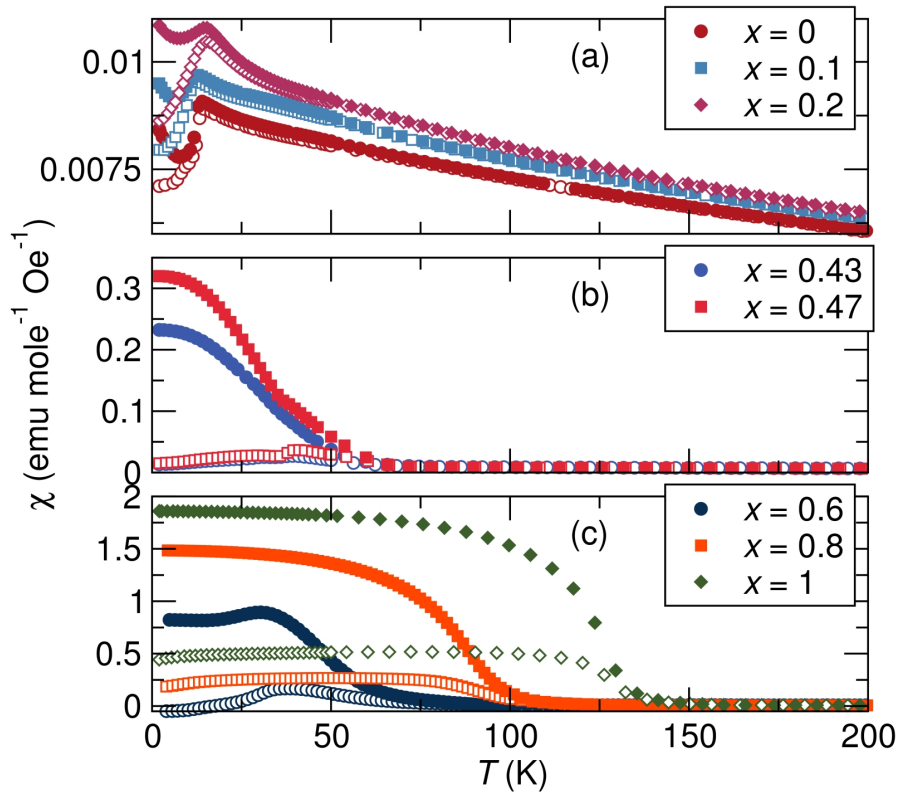


Figure 1. Zero-field-cooled (open symbols) and field-cooled (closed symbols) magnetic susceptibility as a function of temperature of the series $Mg_{1-x}Cu_xCr_2O_4$ under a DC fields of 0.1 T (a) samples with $x < 0.4$, (b) Samples with $0.4 < x < 0.5$, and (c) Samples $x > 0.5$. Magnetic ordering temperatures and the magnetization at low temperatures increase with x concentration.

scattering which verified that all the spinels are normal, meaning the B site is purely Cr^{3+} , and there is not Cr^{3+} on the A site. Magnetic susceptibility measurements on powder samples were performed using a Quantum Design MPMS superconducting quantum interference device (SQUID) magnetometer. In all samples, magnetization as a function of temperature was measured at a field of 0.1 T. Isothermal field dependent magnetization measurements were performed at 2 K and 5 K. A Quantum Design Physical Properties Measurement System was used to measure heat capacity at 0 T for various temperature ranges selected to accommodate the magnetic transition temperature of each sample. For the heat capacity measurements, pellets of 50 % sample mass and 50 % silver mass were prepared by grinding and pressing at about 330 MPa. Silver was used to increase mechanical strength and thermal conductivity. The pellets were mounted on the sample stage using Apiezon N grease. The heat capacity of the grease and of silver heat capacity were collected separately and subtracted to obtain the sample heat capacity.

3. Results and Discussion

We study the magnetic properties of the compounds $Mg_{1-x}Cu_xCr_2O_4$ using magnetic susceptibility measurements. Zero field cooled (ZFC) and field cooled (FC) temperature dependent magnetic susceptibilities of the system show a composition dependent ordering temperature (T_N) defined as the temperature where $d\chi/dT$ is maximum (Figure 1 and Table 3). T_N increases with Cu^{2+} substitution. In addition to Cr^{3+} - Cr^{3+} interactions that are present in all compositions, Cu^{2+} - Cr^{3+} and Cu^{2+} - Cu^{2+} interactions occur in copper doped samples. The increase in T_N correlates well with the increase in the number of magnetic interactions. It is also likely that Cu^{2+} moments compensate some of the Cr^{3+} sublattice moments. As Cr^{3+} are compensated, the difficulty involved with satisfying antiferromagnetic interactions between spins on a pyrochlore lattice is alleviated easing frustration and allowing magnetic order at high T_N . The sample $x = 0.1$ shows a lower T_N suggesting that randomly distributed dilute Cu^{2+} ions may be disrupting long range order, causing the system to freeze into a disordered spin state at lower temperature. The decrease in T_N with dilute doping of magnetic cations on the A site of a frustrated antiferromagnet has been observed in the system $Zn_{1-x}Co_xCr_2O_4$. [34]

In samples $x = 0, 0.1,$ and 0.2 susceptibility increases to a maximum at T_N before decreasing below T_N [Figure 1(c)]. This trend in both ZFC and FC data indicates dominant antiferromagnetic interactions. A sharp cusp is observed at T_N in $MgCr_2O_4$ where long range magnetic order occurs *via* a spin-driven Jahn-Teller transition. [36] This cusp broadens in samples $x = 0.1$ and 0.2 indicating changes in the magnetic ground state with Cu^{2+} doping. Low Cu^{2+} content may contribute to glassy behavior by introducing asymmetric exchange pathways throughout the sample. The decrease in ZFC susceptibility coupled with the increase in FC susceptibility below T_N in compositions $x = 0.43, 0.47, 0.6, 0.8$ and 1 [Figure 1(a) and (b)] demonstrates ferrimagnetic behavior. The magnitude of the low temperature susceptibility increases with Cu^{2+} content as shown in Figure 1.

There are two ordering temperatures in the magnetic susceptibility of samples $x = 0.43$ and $x = 0.47$ (Figure 2, Table 3). This suggests the presence of two different kinds of long range interactions or magnetic compensation. Structural studies of these samples showed that compositions $x \leq 0.43$ have a cubic average structure at room temperature. Under similar conditions, compositions $x \geq 0.47$ showed tetragonal average symmetry. Average cubic and tetragonal symmetry was present in the range $0.43 \leq x \leq 0.47$ at 300 K. Shoemaker *et al.* suggest that although locally CuO_4 tetrahedra are distorted for Cu^{2+} content ≤ 0.43 due to the Jahn-Teller activity of tetrahedral Cu^{2+} , the average structure remains cubic at 300 K. At $x = 0.43$, the distorted CuO_4 distribution is sufficient to cause a cooperative effect and the tetragonal phase appears. [33] Here, magnetic susceptibility studies complement structural studies well. We find that in Cu^{2+} concentrations $x \leq 0.2$, magnetism is antiferromagnetic as occurs in $MgCr_2O_4$. For x above 0.6 , ferrimagnetism develops (Figure 1). Although addition of Cu^{2+} increases ferrimagnetic A - B interactions, antiferromagnetism dominates at low x values. Multiple

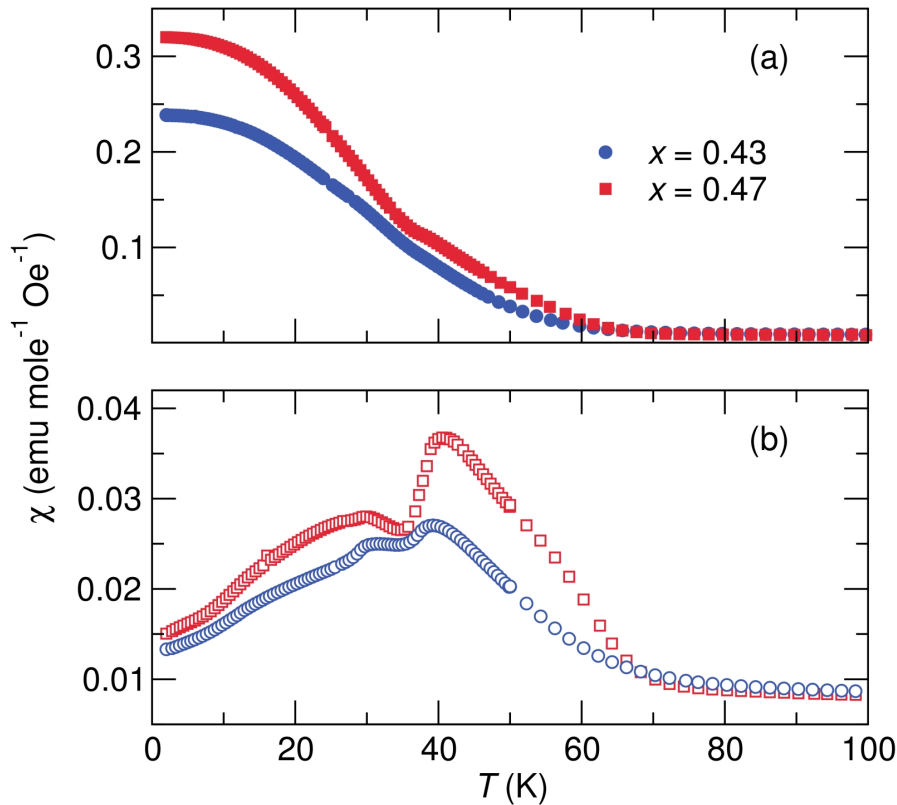


Figure 2. (a) Field-cooled and (b) zero-field-cooled magnetic susceptibility of the compounds with $x = 0.43$ and $x = 0.47$ the showing multiple magnetic transition temperatures present in these samples.

transitions at $x = 0.43$, suggest that A - O - B coupling is sufficient to cause ferrimagnetic (Fi) long range order in addition to antiferromagnetic (AF) order. We attribute the presence of two magnetic transitions in the range $0.43 \leq x \leq 0.47$ to coexisting Fi and AF interactions. Evidence of structural phase separation in the range $0.43 \leq x \leq 0.47$ at 300 K supports the magnetic data showing two distinct yet coexisting kinds of magnetic order.[33] For $x > 0.6$, ferrimagnetism prevails.

High temperature susceptibility data was fit to the Curie-Weiss (CW) equation (Equation 1) to obtain the effective paramagnetic moment (μ_{eff}) and Θ_{CW} .

$$\chi = \frac{C}{T - \Theta_{CW}} \quad (1)$$

The Curie constant (C) yields an effective paramagnetic moment following the expression $\mu_{eff} = \sqrt{3K_B C / N_A}$. Θ_{CW} is a measure of the strength and nature of magnetic interactions. A plot of the scaled normalized inverse susceptibility shown by Equation 2 simplifies comparison of magnetic behavior in compounds where magnetic interactions evolve significantly with composition.[34]

$$\frac{C}{\chi|\Theta_{CW}|} + \text{sgn}(\Theta_{CW}) = \frac{T}{|\Theta_{CW}|} \quad (2)$$

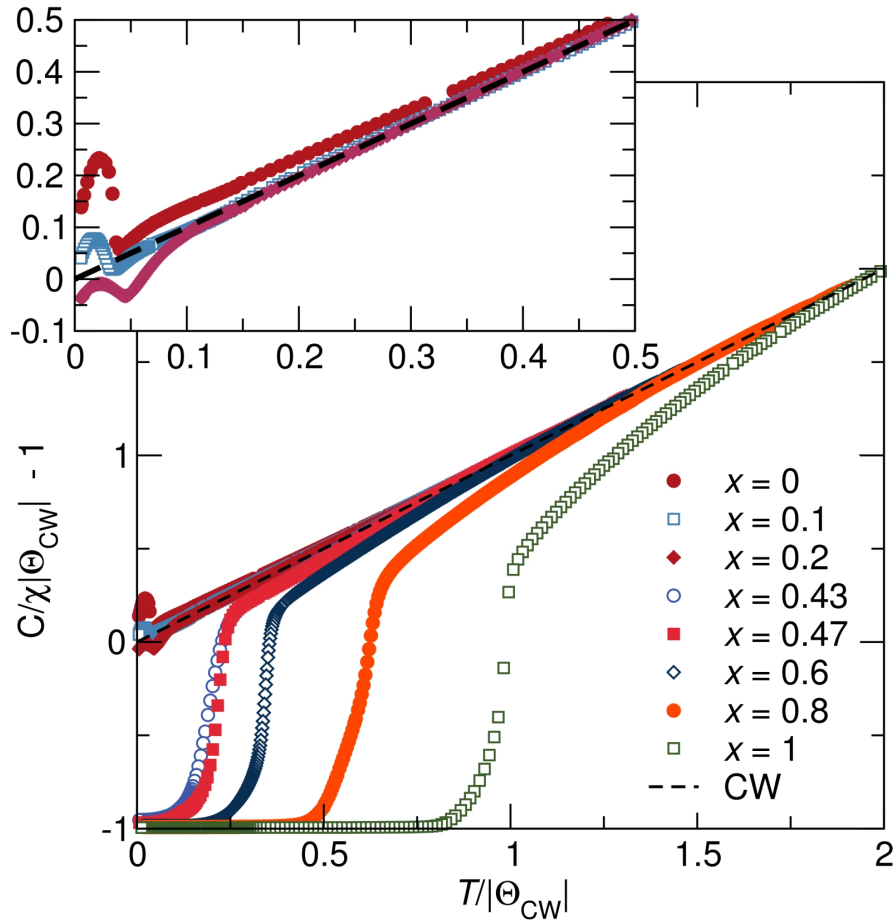


Figure 3. Normalized plots of inverse field-cooled magnetic susceptibility of $Mg_{1-x}Cu_xCr_2O_4$ acquired in a 0.1 T field, as a function of $T/|\Theta_{CW}|$. The black dashed line represents ideal Curie-Weiss (CW) behavior. For small x , the susceptibility follows Curie-Weiss behavior to $T \ll |\Theta_{CW}|$ and at T_N deviate positively from ideal CW behavior as seen also in the inset. Compounds with $x = 0.43, 0.47, 0.6, 0.8,$ and 1 deviate negatively from ideal CW behavior at temperatures closer to $|\Theta_{CW}|$.

Inverse susceptibility scaled according to Equation 2 using values obtained from Curie Weiss fits of the high temperature susceptibility data $300 \leq T \leq 390$ K are presented in Figure 3. Ideal CW paramagnetism occurs in all samples when $T_N/|\Theta_{CW}| \geq 1$ with the exception of $CuCr_2O_4$. In the paramagnetic regime, spins are non-interacting. Deviations from CW behavior denote the onset of long- or short-range interactions. Uncompensated interactions contribute to negative deviations, while compensated interactions lead to positive deviations. Compensated interactions in $MgCr_2O_4$ gradually become uncompensated with Cu^{2+} doping. A neutron study of the magnetic structure of $CuCr_2O_4$ showed that chromium sublattices yield a net moment which is partially compensated by the Cu^{2+} sublattice in the ordered state.[20] It is likely that this effect develops gradually with doping of Cu^{2+} in $MgCr_2O_4$. Deviations from ideal CW behaviour in $CuCr_2O_4$ when $T_N/|\Theta_{CW}| \geq 1$ indicate the presence of short range uncompensated interactions above T_N (Figure 3).

Table 1. Magnetic data of the series $Mg_{1-x}Cu_xCr_2O_4$. Experimental μ_{eff} and Θ_{CW} obtained from fitting susceptibility data in the temperature range $300 \leq T \leq 390$ K to the Curie-Weiss equation. T_N is taken as the temperature where $\partial\chi/\partial T$ is maximum. Calculated spin-only values of μ_{eff} are also presented.

x	μ_{eff} (μ_B , expt.)	μ_{eff} (μ_B , calc.)	Θ_{CW} (K)	T_N
MgCr ₂ O ₄	5.42	5.47	-368	12.5
$x = 0.1$	5.34	5.50	-361	10.5
$x = 0.2$	5.24	5.53	-329	16
$x = 0.43$	5.17	5.59	-314	37, 27
$x = 0.47$	4.94	5.60	-295	38, 29
$x = 0.6$	4.89	5.64	-262	35
$x = 0.8$	4.54	5.69	-202	91
CuCr ₂ O ₄	4.48	5.74	-148	128

The normalized CW plot is a direct indicator of frustrated magnetism. $T_N/|\Theta_{CW}|$ is the inverse of the frustration parameter (f). The onset of long range order when $T_N/|\Theta_{CW}| \ll 1$ is a sign of strong frustration.[37] The canonical geometrically frustrated antiferromagnet, MgCr₂O₄, shows a high frustration index (Figure 3, Table 3). Surprisingly, the compound $x = 0.1$, is the most frustrated of the series despite the presence of random Cu²⁺ ions. Possibly, dilute Cu²⁺ in Mg_{0.9}Cu_{0.1}Cr₂O₄ disrupt Cr³⁺-Cr³⁺ interactions inhibiting the onset of long range order and decreasing T_N . Except for the composition $x = 0.1$, Cu²⁺ doping eases frustration in MgCr₂O₄ and this occurs because of the disruption of symmetric Cr³⁺-Cr³⁺ interactions with random Cu²⁺ distribution in the doped compounds. Cu²⁺ interferes with B - B coupling by adding Cu²⁺-Cr³⁺ and Cu²⁺-Cu²⁺ interactions. Additionally, crystal distortions arise in CrO₆ due to the Jahn-Teller effect of Cu²⁺ depending on proximity to CuO₄ tetrahedra. Differences in Cr-Cr distances and Cr-O-Cr angles due to structural distortions break the degeneracy of exchange coupling routes ultimately easing frustration.

Values obtained from fitting high temperature susceptibility data to the CW equation are tabulated in Table 3 and plotted in Figure 4. An expected spin-only effective moment of series compositions calculated using the expression $\mu_{eff} = \sqrt{x\mu_{Cu}^2 + 2\mu_{Cr}^2}$ is also tabulated. Here $\mu_{eff} = 2\mu_B\sqrt{S(S+1)}$ where $S = 1/2$ and $3/2$ for Cu²⁺ and Cr³⁺ respectively gives the expected effective moment from Cu²⁺ and Cr³⁺. The effective moment is expected to increase with Cu²⁺ concentration. Surprisingly, a decrease in μ_{eff} occurs with Cu²⁺ doping. We speculate that short range interactions develop in the paramagnetic regime in Cu²⁺ rich samples leading to the underestimation of the spin-only effective moment. The orbital contribution to the effective magnetic moment in octahedral Cr³⁺ and Jahn-Teller active Cu²⁺ is expected to be heavily quenched, hence, the orbital moment is not considered.

A negative theoretical ordering temperature (Θ_{CW}) is determined for all samples,

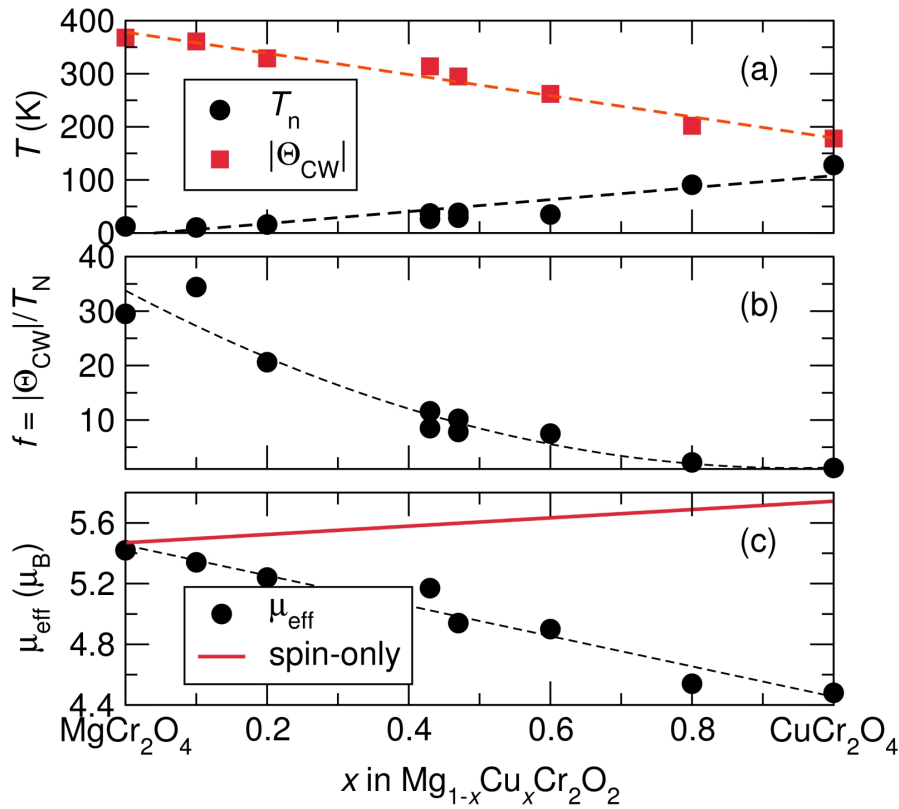


Figure 4. Trends in magnetic properties of $Mg_{1-x}Cu_xCr_2O_4$. (a) T_N increases while Θ_{CW} decreases with x . (b) The frustration index $f = |\Theta_{CW}|/T_N$ decreases with x approaching $f = 1$ as $x = 1$. (c) Experimental μ_{eff} decreases with x although the expected spin-only μ_{eff} is predicted to increase.

confirming that spin coupling is antiferromagnetic or ferrimagnetic. The magnitude of Θ_{CW} decreases with Cu^{2+} content, which is unexpected as Cu^{2+} increases the number of interactions. A similar trend in Curie-Weiss temperature has been reported in the systems $Zn_{1-x}Cu_xCr_2O_4$ [38] and $Cd_{1-x}Cu_xCr_2O_4$. [39] The earlier works postulate that the decrease is due to ferromagnetic interactions from the Cu^{2+} sublattice. Geometry and competition between magnetic interactions results in weaker overall interactions in Cu^{2+} rich samples.

Despite the increase in T_N with Cu^{2+} , the theoretical ordering temperature (Θ_{CW}) shows an opposite trend. Θ_{CW} decreases with Cu^{2+} concentration. The combined change in Θ_{CW} and T_N results in a dramatic decrease of the frustration parameter with Cu^{2+} content. In agreement with previous similar studies [34, 38, 39], we find that frustration is strongly quenched with the addition of spins in the A sublattice. These results show that lattice geometry does not prevent spin order in Cu^{2+} doped samples. The sample $x = 0.1$ exhibits a curious trend. In this compound, the frustration index increases despite Cu^{2+} doping. This was also observed in the study of magnetism of the series $Zn_{1-x}Co_xCr_2O_4$. [34] It is likely that dilute randomly distributed Cu^{2+} introduces disorder in the exchange coupling routes thus disrupting long range order. The system

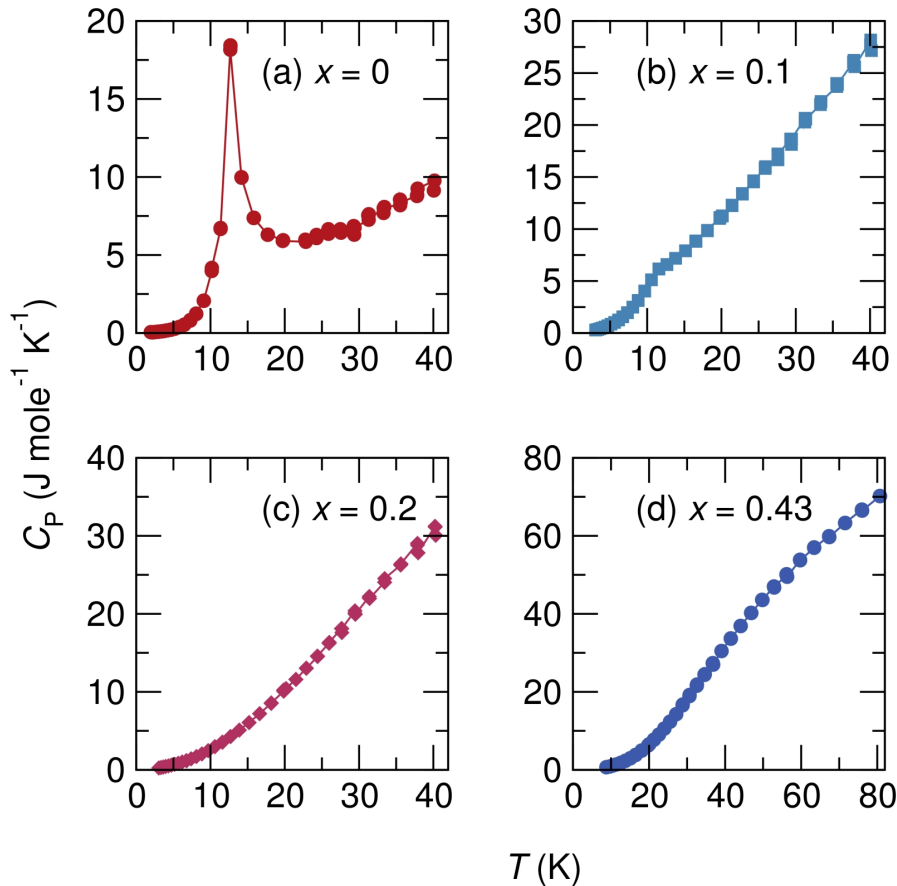


Figure 5. Temperature dependent heat capacity of compounds with $x = 0, 0.1, 0.2,$ and 0.43 in $Mg_{1-x}Cu_xCr_2O_4$ under zero field. (a) Heat capacity of the sample $x = 0$ showing a sharp peak at 12.5 K; (b) A broader peak occurs at 11.5 K in the sample $x = 0.1$; (c) In the samples with $x = 0.2$, a smooth decrease in heat capacity with temperature is observed (d) The sample with $x = 0.43$ displays a broad bulge in the heat capacity at ≈ 50 K.

assumes a frozen disordered state at the suppressed transition temperature.

Entropy changes are well described by specific heat measurements. A sharp peak in the specific heat of $MgCr_2O_4$ indicates changes in entropy at $T \approx 12.5$ K [Figure 5(a)]. The transition temperature recorded in heat capacity coincides with the magnetic ordering temperature signalling the onset of long range AF order. A broad shallow peak at $T \approx 11$ K appears at the magnetic ordering temperature of the sample $x = 0.1$ suggesting that there is a remanent magnetic entropy below the ordering temperature [Figure 5(b)]. The suggestion that for dilute Cu^{2+} concentrations, the spins freeze in a disordered state rather than one with long range order, is further supported by the absence of an anomaly in the heat capacity of the sample $x = 0.2$ [Figure 5(c)]. In the compound $x = 0.43$, a broad hump develops at $30 \text{ K} \leq T \leq 70 \text{ K}$. The broad range in temperature of the transition indicates a more diffuse magnetic transition and the onset of long range order at $x \geq 0.43$ [Figure 5(d)].

A progressive transition from antiferromagnetic to ferrimagnetic order is observed

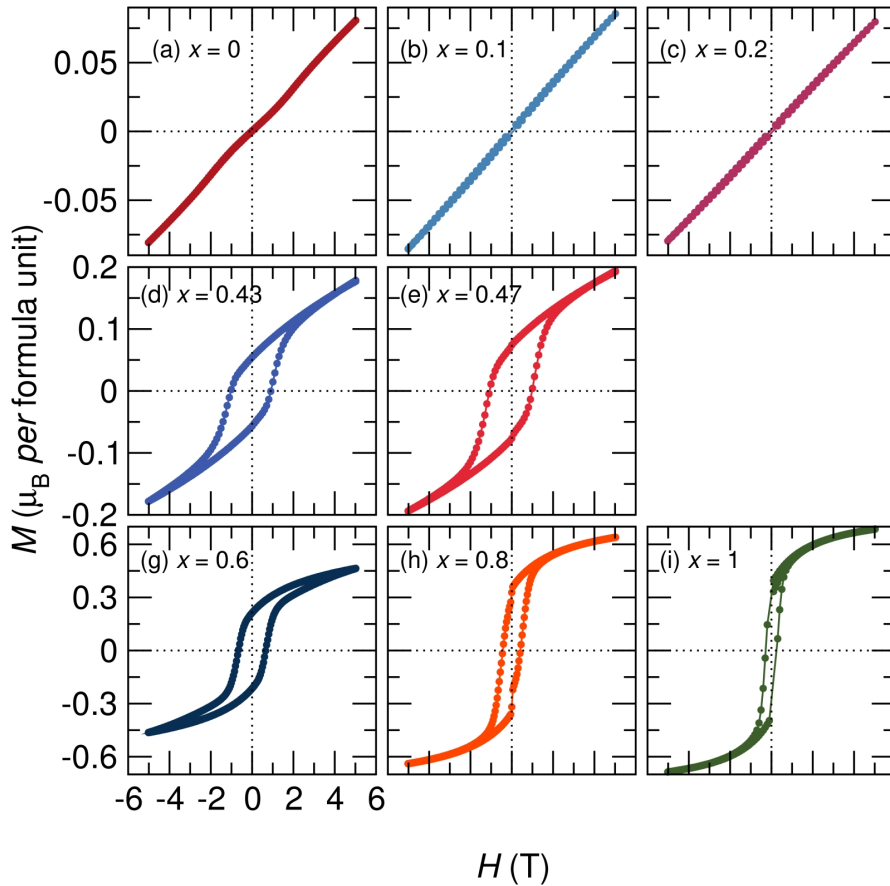


Figure 6. Isothermal magnetization traces of the different $Mg_{1-x}Cu_xCr_2O_4$ compounds, measured at 2 K except for the samples with $x = 0.6$ and 0.8 which were measured at 5 K. The compound (a) $x = 0$ shows a linear variation of magnetization with field. Magnetic anisotropy induces slight nonlinearity at ± 1.5 T as reported by Suzuki *et al.*[?] In (b) $x = 0.1$ and (c) $x = 0.2$ linear dependence of the magnetization on field is again observed. In (d), the $x = 0.43$ sample and in (e) the $x = 0.47$ sample display a larger increase in magnetization as compared to samples with $x = 0, 0.1,$ and 0.2 . A large coercive field develops as observed from the wide hysteresis loops. At high fields the magnetization does not saturate. The samples with (f) $x = 0.6$ and (g) 0.8 are ferrimagnetic with open hysteresis loops and almost saturating magnetization. (h) Field dependence of the magnetization of $CuCr_2O_4$ at 2 K showing well behaved hysteresis and an almost saturated magnetization of $0.7 \mu_B$ per formula unit with small coercive field.

in isothermal field dependent magnetization measurements (Figure 6). In $MgCr_2O_4$, a linear dependence of the magnetization on field that is characteristic of antiferromagnetic order is observed. Slight nonlinearity in the field dependent magnetization develops at ± 1.5 T in $MgCr_2O_4$ [Figure 6(a)]. This nonlinearity originates from a field-driven change in local magnetic structure as postulated by Suzuki *et al.*[?]. Antiferromagnetism persists in samples $x = 0.1$ and 0.2 [Figure 6(b,c)], however, coercivity develops as the loops are open upon close examination. Coercivity is highest in samples $x = 0.43$ and 0.47 [Figure 6(d,e)]. Additionally, earlier studies on exchange bias effects in these

compounds revealed an increase in the exchange bias field (H_e) with Cu^{2+} in samples $x = 0.1, 0.2$ and 0.43 .^[33] Antiferromagnetic-ferrimagnetic interfaces are a common cause of enhanced coercivity and shifted hysteresis.^[40, 41] Given that the samples $x = 0.43$ and $x = 0.47$ bridge the AF and Fi regions, we propose that pinning of spins at the Fi-AF cluster interfaces contributes to the enhanced coercivity.

Coupled with the increased coercivity in compounds $x = 0.43$ and $x = 0.47$ is the change from AF to Fi behavior that is evident in field- and temperature-dependent behavior. In samples with $x = 0.6, x = 0.8,$ and $x = 1,$ the coercivity decreases and the field dependent magnetization becomes ferrimagnetic. $CuCr_2O_4$ has a coercive field (H_e) of about 0.25 T and a saturation moment of $0.68 \mu_B$ per formula unit. The Néel model of antiferromagnetism predicts a saturation moment of $5 \mu_B$ per formula unit in $CuCr_2O_4$. Since the predicted moment far exceeds the measured value, neutron diffraction measurements in the ordered state were used to resolve this discrepancy.^[20] A triangular arrangement of spins explains the low moment. Cr^{3+} on the 001 planes are aligned parallel and opposite to Cr^{3+} in adjacent planes yielding a net moment from the Cr^{3+} sublattices. The Cu^{2+} sublattice couples antiferromagnetically to the net moment of the Cr^{3+} sublattices creating a triangular configuration of spins. A composition dependent saturation magnetization is observed in samples $x = 0.43, 0.47, 0.6, 0.8,$ and $1.$ The saturation moment increases with Cu^{2+} .

We can assemble the $(Mg,Cu)Cr_2O_4$ magnetic phase diagram in Figure 7 by combining magnetic ordering transitions and heat capacity measurements for the various compositions in this study. Transition temperatures specified by anomalies in susceptibility and heat capacity measurements are used to demarcate phase boundaries. $MgCr_2O_4$ enters a long range AF state at $T = 12.5$ K marked by sharp anomalies in both susceptibility and heat capacity. The sharp cusp in the susceptibility of $MgCr_2O_4$ is replaced with a rounded peak in compositions $x = 0.1$ and 0.2 . Although the magnetic order in these compositions is antiferromagnetic as evidenced by the linear dependence of magnetization on field, they possess significant disorder. Disorder is indicated by the suppressed anomaly in heat capacity of the sample $x = 0.1$ and the complete absence of a transition in the specific heat of $x = 0.2$. All compositions $0.2 \leq x \leq 0.6$ exhibit glassy magnetic states. In the sample $x = 0.6,$ ferrimagnetism develops indicated by the similarities in field and temperature dependent magnetization between the compound and the end-member $CuCr_2O_4$. All compositions are paramagnetic above the magnetic transition temperatures.

4. Conclusions

Recent years have seen renewed focus on frustrated magnetic systems as a consequence of the recognition that they can give rise to exotic magnetic ground states.^[37, 42, 43] The introduction of spins in the A site of geometrically frustrated spinels has been suggested as a means of relieving frustration.^[34, 38, 39] We find in agreement with this proposition, that Cu^{2+} alleviates frustration in all $Mg_{1-x}Cu_xCr_2O_4$ compositions studied

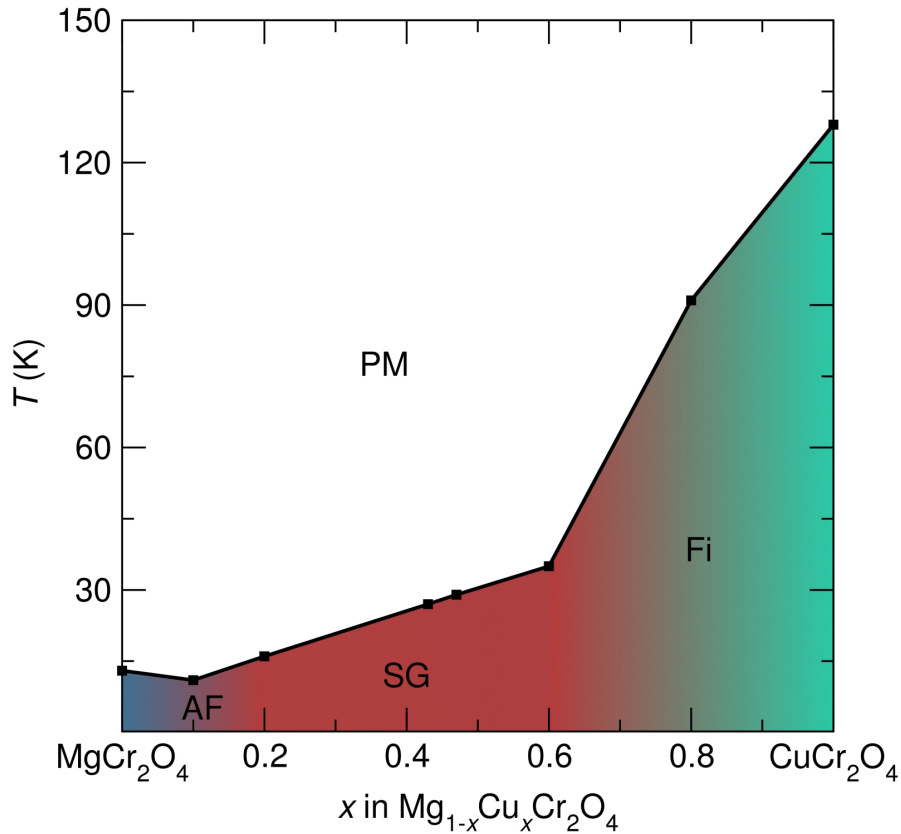


Figure 7. Suggested magnetic phase diagram for the solid solution $Mg_{1-x}Cu_xCr_2O_4$ based on susceptibility, heat capacity and magnetization measurements. In compounds with $x \leq 0.2$, the magnetic ordering is antiferromagnetic (AF) below T_N . For compositions with $0.2 \leq x \leq 0.6$, glassy behaviour (SG) is observed, and for x larger than 0.6, the ordering is largely ferrimagnetic (Fi), albeit not Néel-like.

with the exception of $x = 0.1$. Temperature- and field-dependent magnetization indicate a largely antiferromagnetic ground state in the compositions $x < 0.2$, disordered glassy states with open hysteresis loops in the range $0.2 \leq x \leq 0.6$, and largely ferrimagnetic ground states for $x > 0.6$, albeit with significantly smaller saturation magnetizations than would be found for Néel-ordered states. Specific heat measurements support these conclusions for samples with small x . Emergent behavior at the AF/Fi phase boundary, indicated by large coercive fields and multiple magnetic transition temperatures, suggests microscopic interactions between AF and Fi clusters.

5. Acknowledgements

MCK thanks Joshua Kurzman and Phillip Barton for helpful comments. We gratefully acknowledge support from the National Science Foundation through a Materials World Network grant (DMR 0909180). MCK is supported by the Schlumberger Foundation Faculty for the Future Fellowship. SLM is supported by the RISE program at the Materials Research Laboratory. Use of shared experimental facilities of the

Materials Research Laboratory: an NSF MRSEC, supported by NSF DMR 1121053 is acknowledged. The MRL is a member of the the NSF-supported Materials Research Facilities Network (www.mrfl.org). The 11-BM beamline at the Advanced Photon Source is supported by the Department of Energy, Office of Science, Office of Basic Energy Sciences, under Contract No. DE-AC02-06CH11357.

- [1] Thackeray M M, de Picciotto L A, de Kock A, Johnson P J, Nicholas V A, and Adendorff K T 1986 *J. Power Sources* **21** 1
- [2] Yamasaki Y, Miyasaka S, Kaneko Y, He J-P, Arima T, and Tokura Y 2006 *Phys. Rev. Lett.* **96** 207204
- [3] Lawes G, Melot B, Page K, Ederer C, Hayward M A, Proffen Th, and Seshadri R 2006 *Phys. Rev. B* **74** 024413
- [4] Zhu J, and Gao Q 2009 *Microporous Mesoporous Mater.* **124** 144
- [5] Yaresko A N 2008 *Phys. Rev. B.* **77** 115106
- [6] Glazkov V N, Farutin A M, Tsurkan V, Krug von Nidda H-A and Loidl A 2009 *Phys. Rev. B* **79** 021131
- [7] Ueda H, Katori H A, Mitamura H, Goto T, and Takagi H 2005 *Phys. Rev. Lett.* **94** 047202
- [8] Lee S-H, Broholm C, Ratcliff W, Gasparovic G, Huang Q, Kim T H, and Cheong S-W 2002 *Nature* **418** 856
- [9] Balents L 2010 *Nature* **466** 216007
- [10] Moessner R and Ramirez A P 2006 *Phys. Today* **59** 24
- [11] Dunitz J D and Orgel L E 1957 *J. Phys. Chem. Solids* **3** 318
- [12] Miller A 1959 *J. Appl. Phys.* **30** 4
- [13] Anderson P W 1956 *Phys. Rev.* **102** 4
- [14] Lee S- H, Gasparovic G, Broholm C, Matsuda M, Chung J-H, Kim Y J, Ueda H, Xu G, Zschack P, Kakurai K, Takagi H, Ratcliff W, Kim T H, and Cheong S-W 2007 *J. Phys.: Condens. Matter* **19** 145259
- [15] Moessner R and Chalker J T 1998 *Phys. Rev. Lett.* **80** 13
- [16] Tchernyshyov O, Moessner R, and Sondhi S L 2002 *Phys. Rev. Lett.* **88** 067203
- [17] Kant C, Deisenhofer J, Tsurkan V, and Loidl A 2010 *J. Phys: Conf. Ser.* **200** 032032
- [18] Lawes G, Melot B, Page K, Ederer C, Hayward M A, Proffen Th, and Seshadri R 2006 *Phys. Rev. B* **74** 024413
- [19] Ederer C and Komelj M 2007 *Phys. Rev. B* **76** 064409
- [20] Prince E 1957 *Acta Crystallogr.* **10** 554
- [21] Shirane G, Cox D E, and Pickart S J 1964 *J. Appl. Phys.* **35** 3
- [22] Tomiyasu K, Fukunaga J, and Suzuki H 2004 *Phys. Rev. B* **70** 214434
- [23] Bordács S, Varjas D, Kézsmarki I, Mihály G, Balassarre L, Abouelsayed A, Kuntscher C A, Ohgushi K, and Tokura Y 2009 *Phys. Rev. Lett.* **103** 077205
- [24] Suzuki H and Tsunoda Y 2007 *J. Phys. Chem. Solids* **68** 2060
- [25] Dutton S E, Huang Q, Tchernyshyov O, Broholm C L, and Cava R J 2011 *Phys. Rev. B* **83** 064407
- [26] Ortega-San-Martin L, Williams A J, Gordon C D, Klemme S, and Attfield J P 2008 *J. Phys.: Condens. Matter* **20** 104238
- [27] Ehrenberg H, Knapp M, Baecht C and Klemme S 2002 *Powder Diffraction* **17** 230
- [28] Klemme S, O'Neill H, Schnelle W, and Gmelin E 2000 *Am. Mineral.* **85** 1686
- [29] Kanamori J 1960 *J. Appl. Phys.* **31** S14
- [30] Murthy K S R C, Ghose J, and Rao E N 1983 *J. Mater. Sci. Lett.* **2** 393
- [31] Gerloch M 1981 *Inorg. Chem.* **20** 638
- [32] Dollase W A, and O'Neill H St. C 1997 *Acta Crystallogr., Sect. C: Cryst. Struct. Commun.* **C53** 657
- [33] Shoemaker D P and Seshadri R 2010 *Phys. Rev. B* **82** 214107

- [34] Melot B, Drewes J E, Seshadri R, Stoudenmire E M, and Ramirez A P 2009 *J. Phys.: Condens. Matter* **21** 216007
- [35] Shoemaker D P, Rodriguez E E, Seshadri R, Abumohor I V, and Proffen Th 2009 *Phys. Rev. B* **80** 144422
- [36] Lee S-H, Takagi H, Louca D, Matsuda M, Ji S, Ueda H, Ueda Y, Katsufuji T, Chung J-H, Park S, Cheong S-W, and Broholm C 2010 *J. Phys. Soc. Jpn.* **79** 011004
- [37] Ramirez A P 1994 *Annu. Rev. Mater. Sci.* **24** 1994 453
- [38] Yan L-Q, Macia F, Jiang Z-W, Shen J, He L-H, and Wang F-W. 2008 *J. Phys.: Condens. Matter* **20** 255203
- [39] Yan L-Q, Jiang Z-W, Peng X D, He L-H, and Wang F-W 2007 *Powder Diffraction* **22** 340
- [40] Leighton C, Nogués J, Jönsson-Åkerman B J, and Schuller I K 2000 *Phys. Rev. Lett.* **84** 3466
- [41] Nogués J and Schuller K I 1999 *J. Magn. Magn. Mater.* **192** 203
- [42] Zhang Z, Louca D, Visinoiu A, Lee S-H, Thompson J D, Proffen Th, Llobet A, Qiu Y, Park S, Ueda Y 2006 *Phys. Rev. B* **74** 014108
- [43] Moessner R and Chalker J T 1998 *Phys. Rev. B* **58** 12042